

Collection and spectral control of high-order harmonics generated with a 50 W high-repetition rate Ytterbium femtosecond laser system

A Cabasse, Ch Hazera, L. Quintard, E. Cormier, S Petit, Eric Constant

▶ **To cite this version:**

A Cabasse, Ch Hazera, L. Quintard, E. Cormier, S Petit, et al.. Collection and spectral control of high-order harmonics generated with a 50 W high-repetition rate Ytterbium femtosecond laser system. Journal of Physics B: Atomic, Molecular and Optical Physics, 2016, 49 (8), pp.085601. 10.1088/0953-4075/49/8/085601 . hal-02289956

HAL Id: hal-02289956
https://hal.science/hal-02289956

Submitted on 19 Sep 2019

HAL is a multi-disciplinary open access archive for the deposit and dissemination of scientific research documents, whether they are published or not. The documents may come from teaching and research institutions in France or abroad, or from public or private research centers.

L'archive ouverte pluridisciplinaire **HAL**, est destinée au dépôt et à la diffusion de documents scientifiques de niveau recherche, publiés ou non, émanant des établissements d'enseignement et de recherche français ou étrangers, des laboratoires publics ou privés.

Collection and spectral control of high-order harmonics generated with a 50 W high-repetition rate Ytterbium femtosecond laser system

A. Cabasse, Ch. Hazera, L. Quintard, E. Cormier, S. Petit, and E. Constant

Univ. Bordeaux, CEA, CNRS, CELIA, UMR 5107, F-33400 Talence, France

Abstract: We generate high-order harmonics with a 50 W, Yb femtosecond fiber laser system operating at 100 kHz in a tight focusing configuration. We achieve a high photon flux even with pulses longer than 500 fs. We collect the diverging XUV harmonic beam in a 35 mrad wide solid angle by using a spectrometer designed to handle the high thermal load under vacuum and refocus the XUV beam onto a detector where the beam is characterised or can alternatively be used for experiments. This setup is designed for a 50 eV XUV bandwidth and offers the possibility to perform XUV-IR pump probe experiments with both temporal and spectral resolution. The high-order harmonics were generated and optimized at 100 kHz by using several gas target geometry (a gas jet and a semi-infinite gas cell) and several gases (Argon, Krypton, Xenon) that provide XUV beams with different characteristics. After the spectrometer and for HHG in Xenon, we detect more than $4x10^{10}$ photons per second over 4 harmonics, that is a useful XUV power on target of 0.1 µW. This corresponds to the emission of more than 1µW per harmonic at the source and we achieved similar flux with both the semi-infinite cell and the jet. In addition, we observe a strong spectral selectivity when generating harmonics in a semi-infinite gas cell as few harmonics clearly dominate the neighbouring harmonics. We attribute this spectral selectivity to phase matching effects.

1. Introduction.

Generating ultrashort coherent XUV radiation can now be achieved through high-order harmonic generation (HHG) in gases [Ferray 1988, Mc Pherson] or on solid samples [Borrot 2011]. The unique properties of such an XUV source are very appealing for applications in many domains. The repetition rate of this ultrashort XUV source is of prime importance for many applications and even crucial for coïncidence experiments. Increasing the repetition rate while preserving a high flux of XUV photon per shot is now receiving lot of interest and new laser systems are opening a way toward this goal. Fiber laser systems can now deliver subpicosecond pulses with high average power [Zaouter 2008, Boulet 2009, Eidam 2010] and are compatible with high repetition rate HHG as shown in [Boulet 2009]. Several groups reported HHG with high repetition rate laser systems with the specificity that the moderate energy per pulse imposes a tight focusing geometry for HHG [Lindner 2003, Boulet 2009, Heyl 2012, Hadrich 2011, Cabasse 2012]. Optimization of the XUV emission under these conditions has been considered [Hadrich 2011, Heyl 2012, Cabasse 2012] and an XUV photon flux of 4.5×10^{12} photons/s has been reported by our group after harmonic generation in Xenon using a 10 W fiber chirped pulse amplification (FCPA) system at 100 kHz repetition rate [Cabasse 2012]. Similar results were obtained by other groups and even improved with shorter pulses [Hädrich 2011, Rothhardt 2014] showing that these approaches are getting mature for HHG. It is likely that new high power laser systems will emerge and allow the production of even higher power XUV beams [Krebs 2013, Hadrich 2014, Wang 2014].

Generation of high power XUV beam is important for applications but the recollection, control and delivery of the XUV photons onto experiments is also problematic because of the high XUV beam divergence associated to the harmonic emission in the tight focussing. Similarly, when high order harmonics are generated on solids, a tight focusing geometry is used and the resulting XUV beam is strongly diverging. A second problem associated with these powerful laser systems is the high average power itself. This high thermal load is hard to handle under vacuum as it can easily damage optics.

So far, only the XUV emission conditions have been studied with tight focusing XUV sources and no study have been published on the experimental approaches that can be used to collect the XUV photons and use them despite their high divergence and the high thermal load carried by the fundamental beam. In this article, we describe a compact XUV-IR spectrometer designed to collect the XUV beam over a wide angle (35 mrad) and to image the XUV source (with fine or large spectral selection) onto a detector that can equivalently be a sample to study. This setup can withstand high thermal load as demonstrated with up to 50 W average power from Yb FCPA system. Although not presented here, the setup is also designed to combine the XUV harmonic beam with a delayed IR probe beam in order to perform time resolved pump-probe experiments with high temporal resolution. This spectrometer can be used either as a dispersive component to achieve spectral resolution and focus a given frequency on the sample (or detector) or as a non dispersive component to achieve broadband harmonic transmission and perform pump probe experiments with high temporal resolution.

In the experiment presented here, we performed harmonic generation with a homemade 50 W femtosecond Yb fiber laser system [Nillon 2009] in several targets consisting in a gas jet or a semi-infinite gas cell and several gases (Argon, Krypton and Xenon).

This femtosecond Yb fiber laser operates at a repetition rate of 100 kHz and has a central wavelength of at 1030 nm. We characterized the photon flux at the output of the spectrometer. We also achieve spectral control directly by controlling the interaction geometry. A strong spectral selectivity leading the predominant emission of few harmonics was achieved by using a semi-infinite gas cell and controlling gas pressure and iris diameter.

2. Experimental setup.

The laser system used here is a homemade Fiber Chirped Pulse Amplification (FCPA) laser system [Nillon 2009, Cabasse 2013]. The system is seeded with a Kerr-Lens Mode-locked (KLM) titanium sapphire oscillator emitting 7 fs pulses at 77 MHz. As the oscillator spectrum, centred at 800 nm, spans almost an octave, a weak signal at 1030 nm is used to seed the FCPA Yb laser operating around this wavelength. The first amplifier is a 40 µm core air-clad Yb-doped photonic crystal fiber (PCF) having an inner diameter of 200 µm pumped with a 25 W laser diode emitting at 976 nm. The pulses are then stretched to a duration of 3 ns in a double-pass transmission-grating-based Offner stretcher (density 1750 l/mm). The pulse train passes through two other pre-amplification stages based on the same design and a pulse picker reduced the repetition rate to 100 kHz. The final amplifier is based on a rod-type PCF (80 µm Yb-doped core diameter, 200 µm double clad diameter) and it is pumped with a 200 W fiber laser diode at 976 nm. The amplified pulses are finally recompressed through a two-reflective-dielectric-gratings-based compressor (density 1760 l/mm) with a total efficiency of 90%. The laser system delivers ~ 570 fs pulse duration centred at 1030 nm, with 50 W of average power at 100 kHz repetition rate, resulting in 500 µJ pulse energy. We present in figure 1 the autocorrelation trace and the spatial profile of the amplified pulses. Note that the

autocorrelation shows significant pedestal due to non compensated phase terms that are inherent to the large B integral accumulated in rod type fiber femtosecond amplifiers. Despite this degraded temporal profile, we observed that higher laser power led to higher XUV photon flux via HHG.

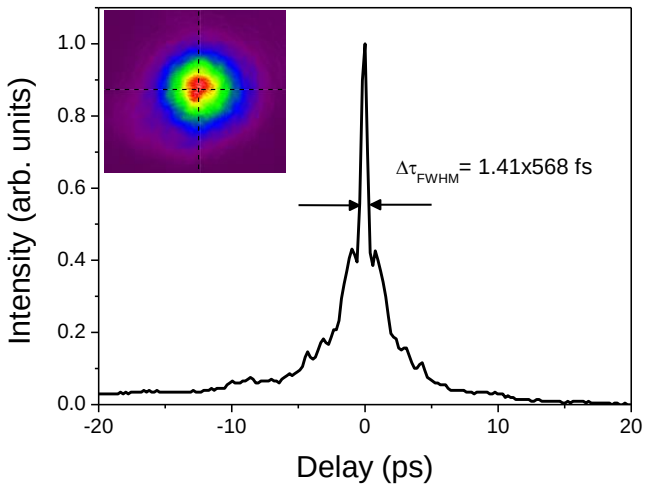


Figure1. Autocorrelation trace of the amplified pulses. Inset: spatial profile of the amplified laser beam.

The 50 W output laser beam is steered through a polarizer, expanded and collimated to a beam size of W = 8 mm (Gaussian like). It is then transmitted through a half waveplate and polarizer to control the pulse energy and ensure that the light is polarized vertically.

The laser beam (M^2 = 1.5) is afterward focused using a 230-mm focal length lens to perform HHG in a dedicated vacuum chamber. The estimated beam size at focus is W_0 = 14 µm and the corresponding confocal parameter is 1.2 mm (Rayleigh length 600 µm). With 50 W average power, the maximum peak intensity is estimated at 2.8×10^{14} W/cm², high enough to perform HHG in gases. The gas is supplied under two different geometries: a continuous gas jet, located at the laser focus, with a nozzle inner diameter of 200 µm or a semi-infinite gas cell (40 mm length) with output located at the focus position. The cell is closed on the entrance side with a window and with a 200 µm thick stainless steel foil on the exit side. A hole is drilled in the foil directly by the laser. Both the gas jet and cell were housed in a vacuum chamber pumped by a turbo pump. The emitted XUV beam is characterized by the XUV spectrometer that was capable to collect the harmonics over a large solid angle. The spectrometer was also designed to separate the harmonics from the fundamental beam with the possibility to recombine then afterward. It could withstand the 50 W average power of the FCPA laser without any damage.

A sketch of the harmonic generation setup and the XUV spectrometer is shown in figure 2. The XUV beam is generated by focusing the femtosecond laser in a first vacuum chamber at the exit of the gas jet or near the exit of the semi-infinite gas cell. The XUV and IR beams are then transmitted through a differential pumping tube (ϕ = 3 mm, L = 30 mm) to a second vacuum chamber containing the spectrometer. The conductance of this tube was small enough to ensure a good pressure difference between the generation chamber (residual pressure up to the 10^{-3} mbar range) and the spectrometer chamber (residual pressure below 10^{-5} mbar) both equipped with a 500 l/min turbo pump.

The IR-XUV interferometer contains two arms. One arm (referred here to as the "spectrometer") collects and refocuses the XUV beam while the other arm is devoted to the control the IR fundamental beam and to recombine IR and XUV beams if needed.

The XUV spectrometer is an imaging spectrometer composed of 4 reflective optics used at ~22.5° grazing incidence (Fig. 2). At the entrance of the spectrometer, the S polarized XUV beam is reflected by a first XUV beam splitter [Falcone 1983, Loch 2011] used at large incidence angle of i = 70° to ensure good reflectivity of the XUV light. The beamsplitter transmits most of the fundamental IR beam and reflects only few percent of the IR beam. This beam splitter is a 10 mm thick SiO_2 plane parallel plate coated with a specific IR anti reflection coating. The AR coating is designed for 1030 nm, 70° incidence and S polarisation and has an external layer (interface to the vacuum) made of Nb_2O_5. This layer ensures a high reflectivity for the XUV over a large bandwidth as its estimated reflectivity [CXRO] is above 40% in the 30 to 80 eV range (Figure 3). The XUV beam is then reflected by a gold-coated toroidal mirror (f = 30 cm, i = 67.5°) located 45 cm after the XUV source, toward a motorized gold-coated flat grating (600 grooves/mm used with an incidence angle close to i = 68.2°). The grating is located 21 cm after the toroidal mirror. The flat grating can be used in its first order for dispersing the beam to characterize it or to use the XUV beam for experiment requiring spectral resolution. It can also be used as a simple mirror at zeroth order to observe the shape of the XUV beam or to perform pump probe experiment with high temporal resolution. Eventually, a second Nb_2O_5 coated beam splitter (identical to the first one) reflects the XUV beam toward the detector (dual microchannel plates equipped with a phosphor screen imaged onto a CCD camera) used to characterize the beam. Alternatively, the detector can be replaced by a sample onto which the XUV beam can be refocused and possibly recombined with a delayed IR pulse transmitted through the second Nb_2O_5 beamsplitter.

The 50 mm diameter beam splitter used at 70° incidence limits the XUV beam width to 17 mm as well as the acceptance angle of the setup (in the horizontal dimension only, the vertical dimension is limited to 50 mm by the splitter aperture). For alignment purpose, an additional 12 mm diameter iris is located in front of the first beam splitter, 34 cm after the XUV source and limits the detection angle to 35 mrad. This iris ensured cylindrical symmetry of the XUV beam.

The spectrometer arm is only used in this paper but the setup enables to recombine the IR and XUV beams for pump probe experiments by using the second delay arm. The IR beam transmitted by the first XUV/IR beamsplitter can then be refocused at the XUV focus. The IR passes through a delay line and is recombined with the XUV beam on the second beam splitter as shown on figure 2. The XUV-IR delay can then be controlled with a motorized delay stage with high accuracy because of the compactness of the setup [loch 2011, Loriot 2015]. The IR intensity at focus could be controlled either with a variable diameter iris or with a half waveplate coupled to a polarizer. This setup is rather compact and the full spectrometer has been installed in a 50 cm diameter vacuum chamber. This compactness is a big advantage for accurate delay control but also for mobility of the full setup [Loriot 2015].

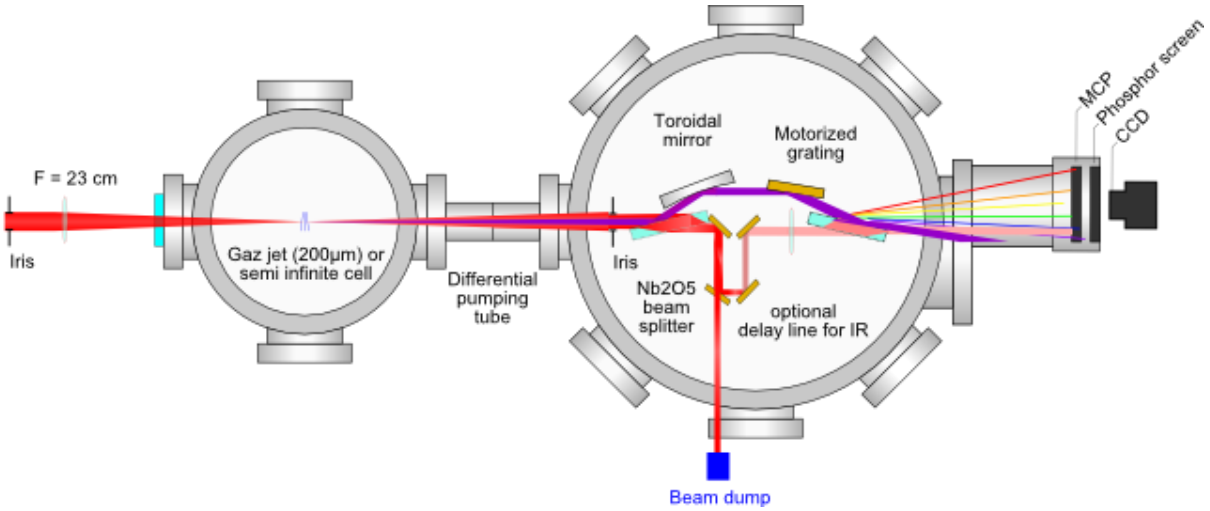


Figure 2. Schematic view of the XUV generation chamber and the wide angle XUV spectrometer with the IR delay arm represented. After HHG, the IR and XUV are split by a grazing incidence XUV beamsplitter and the XUV source is imaged onto a detector with spectral dispersion (first order of the grating) or without spectral dispersion (zero order of the grating). The IR beam can be recombined with the XUV beam to perform pump probe experiments with spectral or temporal resolution with this IR/XUV interferometer.

This setup is designed to cover a large XUV spectral range. Figure 3 shows the theoretical transmission of the XUV spectrometer when the grating is used as a flat mirror (zero order used) in the spectral range 30 eV - 100 eV , by taking into account the reflectivity of the XUV optics (two Nb_2O_5 beam splitters, gold toroidal mirror and gold grating) estimated with tabulated data [CXRO]. For comparison, the SiO_2 reflectivity is also shown on figure 3 as it is now used in many laboratories [Emaury 2015, Hädrich 2014]. In the 30 -100 eV spectral range, it is clearly beneficial to use Nb_2O_5 instead of SiO_2.

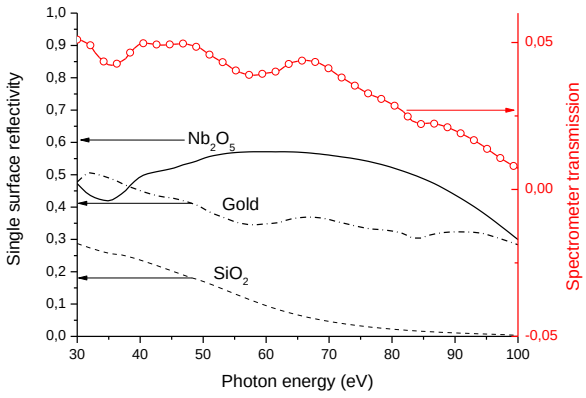


Figure 3. Theoretical reflectivity of the optical elements of the spectrometer: Nb_2O_5 coated beamsplitters (full line) and Gold coated mirrors (dashed line) at 22.5° grazing angle with S polarization. The estimated transmission of the full spectrometer (open circles, right scale) in the spectral range 30 eV – 100 eV for S polarised light and calculated when the gold coated grating is used as a plane mirror (in the zero order).

The spectrometer transmission varies from 6 % at 30 eV to 3% at 80 eV and slightly less than 2% for photon energy of 100 eV. This setup is therefore capable to ensure a transmission of few percent in a large spectral range. It may also be efficient for lower order harmonics but

we could not obtain the refractive index of Nb_2O_5 in the 5-30 eV spectral region. This reflectivity was measured in another experiment and we obtained a reflectivity of ~30 % around 20 eV implying that this setup can also be used for low order harmonics. When the grating is used to disperse spectrally the XUV beam, its diffraction efficiency should also be taken into account to estimate the spectrometer transmission. Note that the transmission of the IR through the first beamsplitter is more than 82 % and the combination of both provides attenuation larger than 97 %. This attenuation is sufficient to block the remaining IR light with an Al filter even when the zero order of the grating was used. By using the grating in its zero order, we could insert an Al filter (Luxel Al filter, 150 nm thick) after the second XUV beamsplitter and we observed that the filter could withstand the remaining IR power without damage. This also allows us to observe the XUV beam with the zero order of the grating with the MCP detector and to measure the XUV photon flux with an XUV photodiode. This confirms that after proper attenuation of the fundamental via grazing incidence reflection, the high initial thermal load remains compatible with the use of standard XUV optics without damage.

The grating used here has a constant groove density while the incoming XUV beam is converging on the grating. This induces some aberrations in the dispersive imaging system as the incidence angle changes with position on the grating. Thus, a monochromatic beam would be diffracted by the grating in a position-dependent manner leading to limited spectral resolution. The beam is approximately 14 mm wide on the toroidal mirror and, for a 75 cm distance between the toroidal mirror and the image, this implies that the XUV beam has a divergence of $\delta i = +- 9\ 10^{-3}$ mrad. This angular spread limits the achievable spectral resolution in the image plane. To estimate this spectral resolution, we use the grating formula:

$$\sin(i) - \sin(r) = \lambda/d \quad (1)$$

with *i* the incidence angle, *r* the diffracted angle and d the groove spacing.
By differentiating this formula for a monochromatic radiation we obtain:

$$\cos(i)\ \delta i = \cos(r)\ \delta r \quad (2)$$

That leads to $\delta r = \cos(i)/\cos(r)\ \delta i$. For a total deviation of 137.12°, the incidence angle is i ~ 68° and the diffracted angle is similar. Therefore an angular spread of few mrad is induced by the geometric aberrations of the setup.
This angular spread is clearly a limitation in our experiment. The achieved spectral resolution is not sufficient to study the harmonic spectral width. It is nevertheless sufficient to discriminate between harmonics. If higher spectral resolution is required, this limitation can be circumvented by using a dedicated XUV grating with variable grove density [Poletto 2004]. This approach would not reduce the photon flux as compared to the setup presented here and would lead to a much better spectral resolution. With a grating with constant groove density, spectral resolution can also be increased by inserting a rectangular aperture (a slit) before the grating to limit the XUV beam divergence perpendicularly to the groove direction. By controlling the number of illuminated grooves that impacts the pulse stretching after diffraction, a slit also provides a way to control continuously the temporal stretching imposed by the grating when used in the first order but inserting a slit also reduces the overall XUV signal. Therefore, when an improved spectral resolution is needed, it would be beneficial to use gratings with a variable groove density. This was not done here as the resolution was sufficient to discriminate the harmonics.

3. Experimental results

Despite the four reflexions in the spectrometer, the XUV detector is easily saturated when located in the image plane. Observing the XUV beam outside of the image plane is beneficial to avoid saturation of the dual MCP detector. To avoid saturation, the MCP voltage is reduced

to ~1200 V (instead of the 2000 V nominal value) and the MCP are moved 5 cm after the image plane to enlarge the XUV beam. This displacement further reduces the spectral resolution that remains sufficient to discriminate between harmonics.

We observed high order harmonics and recorded the XUV spectra emitted both in a gas jet and a semi-infinite gas cell, in Argon, Krypton and Xenon. In a gas jet, the highest order harmonic observed in Argon was H31. It was observed both in Argon and Krypton. We have also produced and detected harmonics up to H23 in Xenon. The lowest harmonic observed was the 7th but for these low orders, harmonics are hardly resolved (significant overlap with neighbour harmonics and second order) and their observation would require reducing the divergence of the XUV beam on the grating.

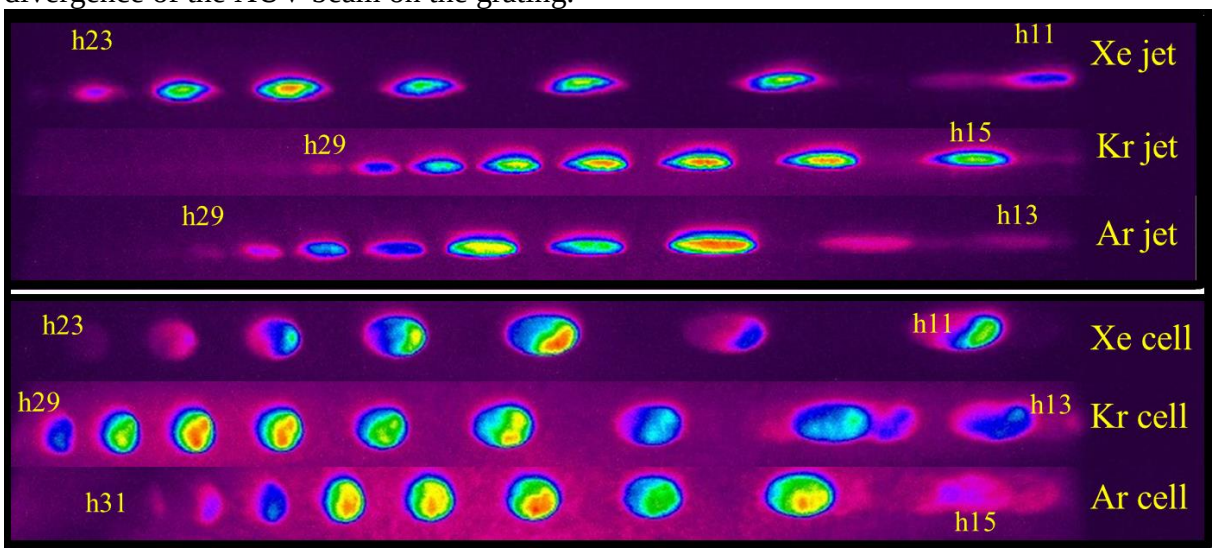


Figure 4. Harmonic spectra observed after emission in a gas jet (top 3 figures) with MCP detector located in the image plane or after emission in a semi infinite gas cell (lower 3 figures) with MCP detector located 5cm after the image plane. The maximum orders observed were 23 for HHG in Xenon and 31 for HHG in Ar or Kr.

With a semi-infinite gas cell, odd harmonics have been produced in Argon (up to H31), Krypton (up to H31) and Xenon (up to H25).
The maximum orders observed were similar with both jet and cell. It indicates that the observed cutoff position was mainly imposed by the single atom response or by the transmission of the spectrometer but not by propagation effects in the generating medium.

In this case, the cutoff position can provide an estimate of the intensity at which harmonics are produced. The cutoff law [Lewenstein 1994, Corkum 1993], $h\nu_{max} = I_p + 3.2\ U_p$ with U_p = 10 eV for I = 10^{14}W/cm^2 at 1030 nm (photon energy is 1.2 eV) gives a maximum intensity of $5x10^{13}$ W/cm^2 for HHG in Xenon and of $7x10^{13}$ W/cm^2 for HHG in Ar and Kr. These values are smaller than the estimated peak intensity and it can indicate that the peak intensity was initially overestimated. It can also indicate that HHG occurs before the maximum of the pulse and is prevented afterwards when the atoms get ionized. This ionization occurs at low intensity with long pulses but if the ionization were a limiting effect, a clear difference in the maximum cutoff order should be observed between HHG in Ar and in Kr which is not the case here.

It is also possible that the XUV spectrometer transmission decreases abruptly above 37 eV. The theoretical estimate shown in figure 3 does not support this possibility when the roughness of the optics is neglected but this discrepancy could be due to their roughness that has an increasingly important impact for short wavelength. We tried to perform HHG in Neon to observe the spectral response of the spectrometer over a broader spectral range but we could not observe any harmonics, suggesting that the peak intensity was too low to perform HHG in Neon.

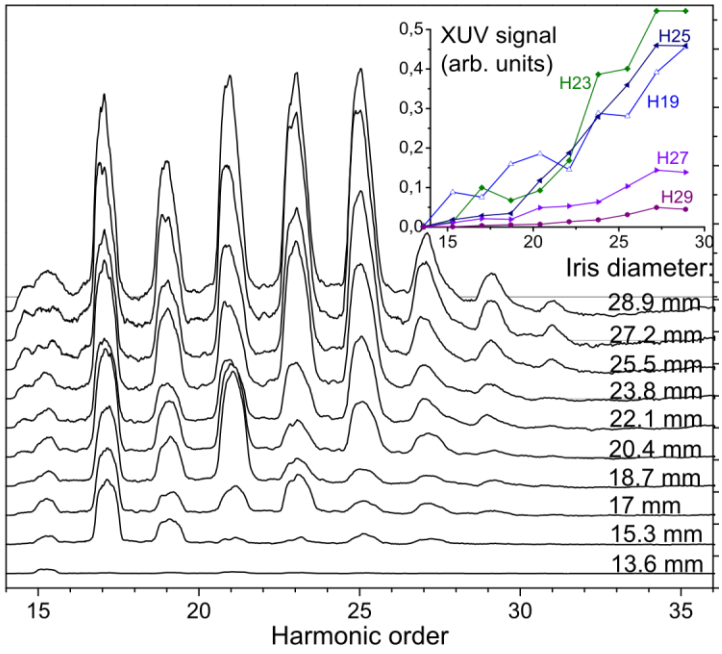


Figure 5. Harmonic spectra observed after HHG in a semi infinite Argon cell for several values of the iris diameter (from bottom to top, iris diameter = 13.6 mm, 15.3 mm, 17 mm, 18.7 mm, 20.4 mm , 22.1 mm, 23.8 mm, 25.5 mm, 27.2 mm and fully open). Inset: Evolution of the integrated signal as a function of the iris diameter.

To disentangle all these possibilities, we studied the harmonic signal generated in Argon as a function of the diameter of an iris that was located before the focusing lens (see figure 1). Closing the iris increases the beam waist at focus and reduces the peak intensity in the generating medium.

We observed (figure 5 a) that the cutoff position was strongly dependent on the iris diameter and that the cutoff position regularly decreased when the iris was closed. It should remain unchanged if the cutoff position was imposed by the ionization at saturation intensity and remain at a constant value provided that the peak intensity is above the saturation intensity. We also observed that the amplitudes of the cutoff harmonics decreased regularly when the iris was closed (fig 5b). If the intensity in the medium was too strong with the fully opened iris, they would increase because of volume effect when we close the iris. Both observations imply that the apparent intensity is not limited by ionization of the atoms. We conclude therefore that the peak intensity in the Ar medium is correctly estimated with the cutoff law and is on the order of $7x10^{13}$ W/cm^2. It should also be the case in Kr where the same maximum order is observed but not in Xenon where ionization must limit harmonic generation before the peak of the pulse.

After optimization, the observed harmonics photon fluxes were similar with the gas jet and semi infinite cell when we detected all the harmonics that were transmitted by the Al filter. It was slightly higher when the jet was used in agreement with [Heyl 2012] but only by a factor smaller than 2. The spectra were however influenced by the pressure in different ways in these two geometries. With the gas cell, saturation was easily reached at low backing pressure and a maximum XUV signal was obtained with a backing pressure of few 100 mbar. With the gas jet, the XUV signal was increasing with the backing pressure and a saturation was only obtained for the lowest harmonics at the highest pressure we could use (~1 bar backing pressure). For the higher harmonic order, no saturation could be reached within the pressure range that the turbo pump can withstand. Note that specially designed gas nozzles allowing HHG extremely close to the nozzle exit have been used in an other group to achieve saturation [Rothhardt 2014] but such nozzles were not available here. Instead, when the laser beam gets too close to our nozzle exit, it eventually melts the glass nozzle thereby preventing HHG.

To further characterize the performances of this compact XUV beamline, we measured the XUV photon flux after the spectrometer for all harmonics above order 15. For this measurement, the XUV grating was used in its zero order to redirect the XUV beam directly onto the detector. The photon flux was measured by inserting an XUV photodiode (Silicon photodiode XUV-100 from UDT sensor) shielded with two aluminium filters after the second XUV beam splitter. The signal measured with the photodiode coupled to a pico-amperemeter is plotted on figure 6 as a function of the Xenon backing pressure.

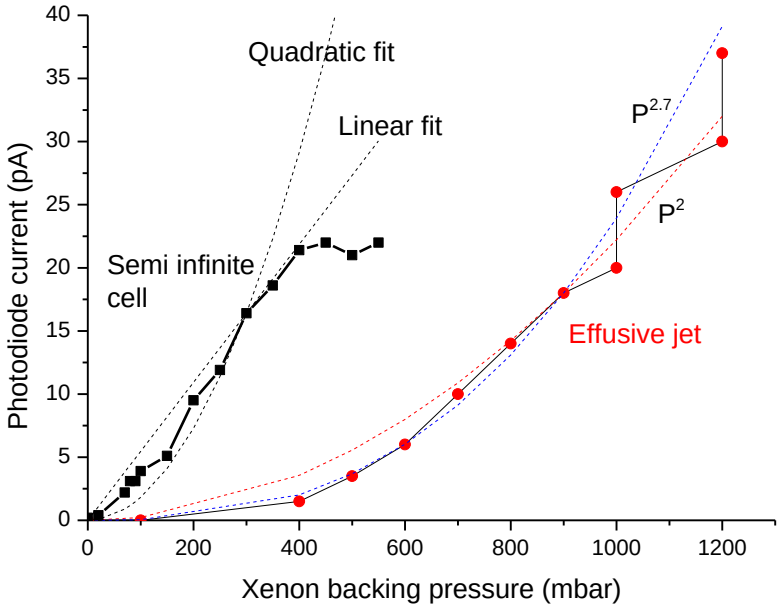


Figure 6: Current emitted by the XUV diode shielded with two aluminum filters as a function of the Xenon backing pressure.

We observed on figure 6, that the optimized numbers of detected XUV photon was similar when harmonics were generated with the jet or the semi infinite gas cell. The photon flux strongly evolved with the gas pressure.
As the number of detected photons could be measured over a large range of pressures, we could fit the data by a power law (Fig. 6). In both case, the P^2 fit led to a poor approximation

of the experimental data. This is expected as the P^2 law is only valid if one considers a constant interaction geometry where only the number of emitters changes with pressure [Kazamias 2011, Heyl 2012]. The gas pressure can affect the signal in other ways such as modification of the coherence length that impacts phase matching [Rundquist 1998] or modification of the emitting volume induced by reabsorption of the harmonics [Constant 99, Mevel 00].

For the jet, we obtained the best fit by using a power law with a non linearity factor of 2.7 for backing pressure below 1 bar. This implies that the output signal is not only affected by the total number of emitters but also that it is influenced by propagation in the medium. A non linearity factor larger than two implies that the phase matching conditions get improved at higher pressure and it is consistent with the explanation formerly given by [Kasamias 2011]. For high pressure, the non linearity order seems to decrease and this indicates that a saturation occurs as is often the case when absorption or off-axis emission gets important [Constant 99, Mevel 00].

For the semi-infinite gas cell, we observed that the signal evolution laid between a linear and a quadratic function of the pressure. Saturation is reached rather quickly and a careful observation reveals slight oscillations of the signal with the pressure. This complex behaviour leading to oscillations in the signal had been anticipated in recent papers [Steingrube 2009, Cabasse 2012, Rothhardt 2014]. Steingrube and Cabasse outlined the impact of propagation and absorption in the medium and also noted that the focus position has a major impact on the evolution of the output signal. Phase matching is also expected to modulate the efficiency [Rothhardt 2014, Heyl 2012] but it usually exhibits a single predominant maximum when on axis phase matching is achieved in a 1 D configuration. Multiple oscillations have also been observed and attributed to Maker fringes [Heyl 2012, Kazamias 2003]. This rich evolution is particularly complex in a semi-infinite cell and deserves to be measured after a complete characterization of the beam near the focus. A specific parametric study will be performed in an other dedicated experiment since the focus position and beam characteristics are specifically important to estimate the HHG efficiency in the semi-infinite cell geometry [Sutherland 2004, Brichta 2009]. Here we mainly focussed on optimizing the XUV signal after the spectrometer and the focus position was only known with a mm accuracy as it is difficult to characterize perfectly this position with tight focusing and short confocal parameters.

The photodiode signal was analysed to estimate the number of XUV photons at the output of the spectrometer. The signal recorded with a pico amperemeter had a maximum value of 30 pA when the two Al filters were used.
The measured transmission of one aluminium filter was 3% for h19, 5% for h21 and 8% for h23. The transmission was estimated with the spectrometer (spectra measured with and without Al filter) and it was not measured for lower harmonics (h15 and h17) because of the overlap between the first and second order of diffraction in this range.
The measured 30 pA current ($I = 30 \times 10^{-12}$ Cb/s) emitted by the photodiode is a current of 1.88×10^8 electrons/sec.
One photon of the 15^{th} harmonic (resp. 21^{st}) has an energy of 18 eV (25.2 eV). By considering that an energy of 3.63 eV is needed to create one electron in the photodiode as stated by the company as a typical photodiode response, we deduce that one XUV photon from the 15^{th} harmonic generates 5 (resp. 6 for h21) electrons. For the measured harmonics (order 15-17-19-21), we assume that the absorption of one XUV photon creates on average 6 photoelectrons. Therefore, we estimate that approximately 3.1×10^7 photons / sec are detected

by the photodiode after the spectrometer and the two Al filters. By cross calibrating our photodiode response with a calibrated photodiode on the LaseriX facility (Courtesy S. Kazamias, K. Cassou and collaborators), we observed that the sensitivity of our XUV photodiode was 3 times lower than the predicted value. We therefore estimate that $9x10^7$ photons were detected by the photodiode each second. By considering a 3% transmission for each Al filter, we estimate that 10^{11} photons per second are transmitted by the spectrometer (*ie* cross the interaction zone before the Al filters) or ~$2.5x10^{10}$ photons per harmonic per second as these photons, generated in Xenon, are mainly contained in 4 harmonics (with order 15-17-19-21). This estimate gives the number of photons transmitted by the spectrometer and this number is high enough for many applications. By considering that the spectrometer transmission is on the order of a percent, approximately 10^{12} photons per harmonic per second should be generated. This number is consistent with previously published values [Cabasse 2012, Hadrich 2011].

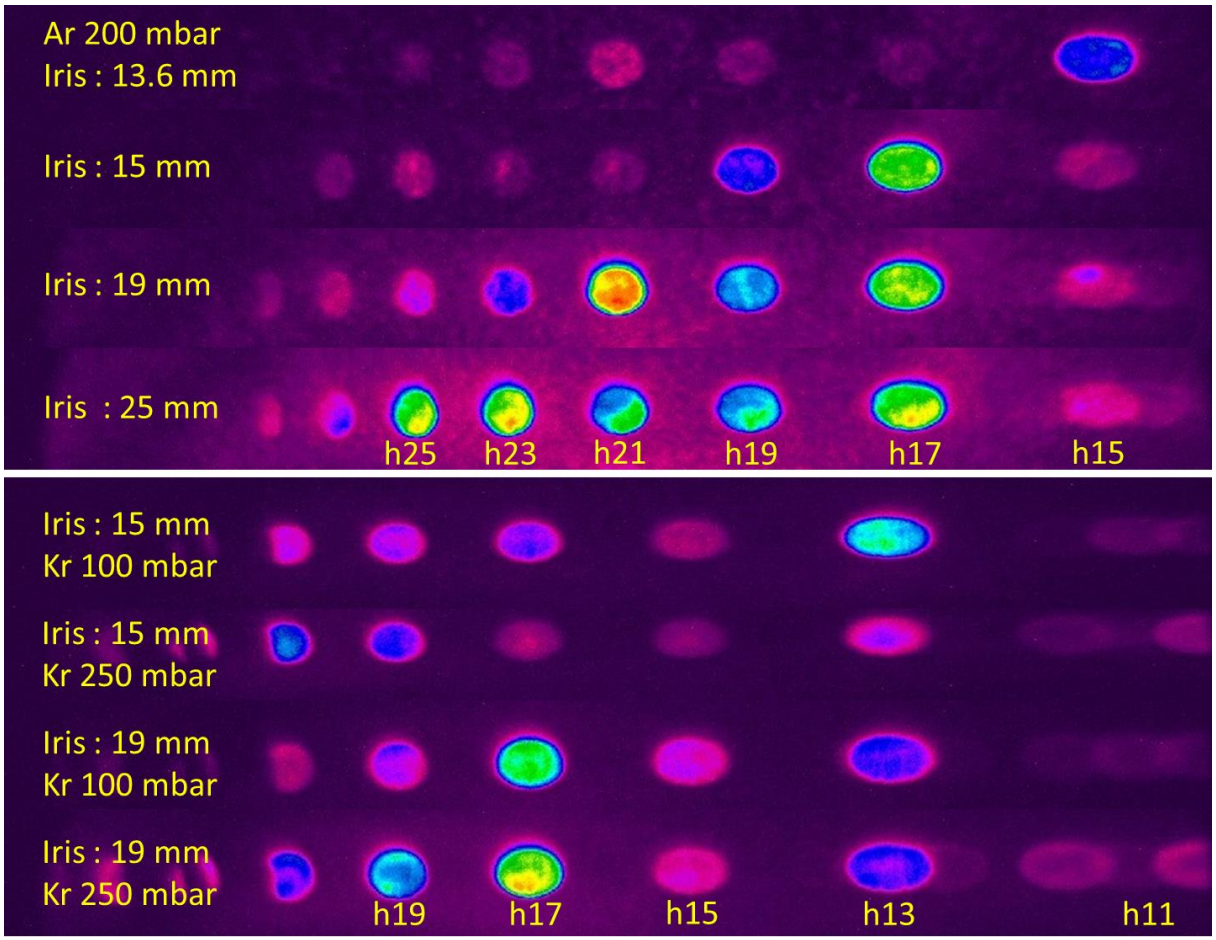


Figure 7. Evolution of the XUV spectra for several diameters of the iris after HHG in Argon at 200 mbar (top 4 figures) or Krypton (down 4 figures) for several pressures (100 and 250 mbar) and iris diameter (15 and 19 mm). A spectral reshaping leading to the selection of few predominant harmonics is observed.

We also observed that propagation in the semi-infinite gas cell could lead to a clear spectral shaping and that the spectral content of the XUV beam could significantly change with the

gas pressure and the beam size. Figure 4 and 7 show that some harmonics generated in the cell can be significantly stronger than the neighboring harmonics for some specific pressures and interaction geometries controlled by the iris diameter and focus position. The harmonic signal changed significantly with the harmonic order with the semi-infinite cell. The signal could change by more than a factor 3 between the main harmonic and its neighbors.
This behavior can be interesting for "automatic" spectral selection [Winterfeldt 2008] and large effort are currently devoted to the selection of isolated harmonics [Wang 2014]. This harmonic selectivity was strong and reproducible when the semi-infinite gas cell was used. It was much less pronounced when harmonics were generated in a gas jet and all the harmonics had similar amplitudes in this case. This observation implies that propagation plays an important role in this spectral shaping. It is likely due to order dependent phase matching with best phase matching (wave vector mismatch, $\Delta k \sim 0$) for one harmonic and with poor phase matching (non-zero wave vector mismatch) for the neighboring harmonics. As only the effective length, L, of the generating medium was changing between jet and cell, observing a similar signal level in both cases is consistent with the fact that large wave vector mismatch, $\Delta k \neq 0$, are compatible with high harmonic flux when small generating media (jet) are used (Δk L being the relevant parameter that determines the macroscopic efficiency in a 1D approach). At the opposite, long media (such as a semi-infinite gas cell where the effective medium length is on the order of the confocal parameter) require smaller wave vector mismatch to lead to efficient on-axis emission. For long media, small variation of Δk from one harmonic to the next can lead to significant modulation in the harmonic signal. It leads to efficiency modulation from one harmonic to the next and spectral selectivity as observed here. The observed selectivity seems to be more pronounced than the selectivity achieved with a semi-infinite cell and high harmonics generated with an 800 nm laser [Brichta 2009, Sutherland 2004] or at larger wavelength where group of harmonics can be enhanced [Popmintchev 2008, Rundquist 1998]. This enhanced selectivity can be related to the central fundamental wavelength (1030 nm) and the moderate order harmonics considered here. Indeed, for a given intensity, the ponderomotive energy is higher at 1030 nm than at 800 nm. This large ponderomotive energy allows generating HHG at 1030 nm at low intensities before a significant ionization occurs while generating an identical XUV frequency with a 800 nm fundamental pulse requires an higher intensity that leads to a stronger ionization. Therefore, the ionization can be more significant at 800 nm than at 1030 nm and it is known that ionization washes out the phase matching effects by inducing space & time dependent phase matching [Constant 1999]. This spectral selectivity should also arise at fundamental wavelength larger than 1030 nm as presented in [Popminchev 2008]. However, when the fundamental wavelength increases too much, the harmonics are getting spectrally closer and the relative index changes gets smaller between neighboring harmonics thereby selecting a group of harmonics instead of individual harmonics. A fundamental wavelength close to 1 µm seems therefore to be an interesting trade-off for selectivity of a single harmonic. Note that despite of the small ponderomotive energy difference between 800 nm and 1030 nm (~1.6 for a given intensity), the generation of a given XUV frequency require intensities that are very different with these two central wavelengths. Generation of 30 eV photons via HHG in Kr requires an intensity of 8×10^{13} W/cm^2 for a pulse centered at 800 nm and only 5×10^{13} W/cm^2 for a pulse centered at 1030 nm. The ionization rates of krypton at these intensities are very different and its estimation with the ADK rate gives values of 4×10^{11} s^{-1} and 10^{10} s^{-1}. For a 500 fs pulse, this leads to an ionization rate of 20% with an 800 nm pulse and only 0.5% with the 1030 nm pulse. It is known that free electrons are highly dispersive and it is usually accepted that an ionization rate of few percent can significantly change the phase matching conditions. Therefore ionization is deleterious to observe well defined phase matching

conditions with a pulse centered at 800 nm while for a pulse centered at 1030 nm ionization is almost negligible.
In other words, at the appearance intensity required to generate XUV photons with a 30 eV energy via HHG in a Krypton gas, a 500 fs pulse centered at 1030 nm leads to the same ionization yield as a 12 fs pulse centered at 800 nm. This implies that at 1030 nm, long pulse duration are still compatible with moderate order harmonic generation with a little ionization while this is not the case for 800 nm pulses.
Our observations also benefits from the high repetition rate of the laser used here since a significant photon XUV flux can be emitted at high repetition rate even under conditions where the signal per pulse is rather low *i.e.* at the low intensities used here.

To be more quantitative on the impact of phase matching, one can consider an effective emission length of 1.3 mm (twice the Rayleigh length) when the semi-infinite cell is used. With this length, it is sufficient to have an index changing by $2x10^{-5}$ from one harmonic to the next to pass from a phase matched situation to a non-phase matched situation. The rare gas index are not known below 30 eV but such a small index difference between two harmonics frequencies seems to be realistic as it is typically the value obtained at 100 – 200 mbar around a photon energy of 30 eV [CXRO] in Ar or Kr.
We note that the spectral shaping evolved strongly with the iris diameter that defines the geometrical phase advance and can ensure good phase matching for a given harmonic but it only changed weakly with the gas pressure (figure 7). The selectivity also gets weaker at high intensity where ionization can start to impact phase matching and at high pressure where the effective medium length can be reduced by the absorption.

4. Conclusion and perspectives

We presented the combination of a high average power Yb fiber laser and an XUV generation and detection setup devoted to harmonic recollection over an angle as large as 35 mrad. This ensemble is compatible with the high thermal load of the 50 W fundamental Yb laser used in the experiments. It provides then a unique source for coherent control and ultrashort XUV light at very high repetition rate (100 kHz up to few MHz). It is also compatible with pump-probe experiments at high repetition rate required for coincidence experiments. The number of detected XUV photons was high. We obtained $4x10^{10}$ photons per second at the output of the setup when harmonics were generated in Xenon and when all harmonics above the 15^{th} were refocused on the detector. We stress that this corresponds to a number of photons that can be effectively used for experiments. As the transmission of our setup is of a few %, the number of generated photons must be in the range of 10^{12} photons per harmonics per seconds and leading to an estimated flux of 1- 10 µW per harmonic similar to the flux measured formerly [Cabasse 2012, 2013, Haddrich 2011, 2014]. We also observed that the pulse duration is not detrimental for high power HHG with Yb laser and using ~ 500 fs, 1030 nm fundamental pulses is compatible with a high XUV photon flux. This setup allowed us to observe that similar photon flux could be obtained with a jet or a semi-infinite gas cell but the gas load is strongly reduced with a gas cell. We observed that the generating conditions are strongly dependent on the gas pressure and the iris diameter. When a semi infinite gas cell was used, controlling these parameters could lead to a clear spectral shaping and to the generation of few predominant harmonics.

We acknowledge stimulating discussions with E. Mével, D. Descamps, V. Strelkov, A. Marciniak, V. Loriot, F. Lépine and F. Catoire and thank K. Cassou, O. Guilbaud, S. Kazamias for their help in cross-calibrating the XUV photodiode.

We acknowledge support for the Region Aquitaine (20101304005, 20131603008 20051304002AB, 20061304003 and 20091304002), from the Agence Nationale de la Recherche (ANR-09-BLAN-0031-02) and from the European community (Laserlab III with GA-284464).

References:

[Borot 2011] Antonin Borot, Arnaud Malvache, Xiaowei Chen, Denis Douillet, Grégory Iaquianiello, Thierry Lefrou,Patrick Audebert, Jean-Paul Geindre, Gérard Mourou, Fabien Quéré, and Rodrigo Lopez-Martens
"High-harmonic generation from plasma mirrors at kilohertz repetition rate"
Optic letters **36**, 1461 (2011).

[Boulet 2009] Johan Boullet, Yoann Zaouter, Jens Limpert, Stéphane Petit, Yann Mairesse, Baptiste Fabre, Julien Higuet, Eric Mével, Eric Constant, and Eric Cormier
"High order harmonic at MHz level Repetition Rate Directly Driven by an Yb Doped Fiber Chirped Pulse Amplification System", Optics Letters **34**, 1489 (2009).

[Brichta 2009] J.-P. Brichta, M.C.H. Wong, J. B. Bertrand, H.C. Bandulet, D.M.Rayner, and V.R. Bhardwaj
"Comparison and real time monitoring of high order harmonic generation in different sources", Phys. Rev. A **79**, 033404 (2009)

[Cabasse 2012] A. Cabasse, G. Machinet, A. Dubrouil, E. Cormier and E. Constant
"Optimization and phase matching of fiber laser driven high-order harmonic generation at high repetition rate », Optic Letters **37**, 4618 (2012).

[Cabasse 2013] A. Cabasse, G. Machinet, C. Hazera, S. Petit, E. Cormier, and E. Constant
"Optimized XUV source at 100 kHz repetition rate", EPJ Web of Conferences **41**, 01015 (2013).

[Constant 1999] E. Constant, D. Garzella, E. Mével, P. Breger, Ch. Dorrer, C. Le Blanc, F. Salin and P. Agostini
"Optimizing High Harmonic Generation in Absorbing Gases : Model and Experiment", Phys. Rev. Lett. **82**, 1668 (1999).

[Corkum 1993] P. B. Corkum
Plasma perspective on strong field multiphoton ionization
Phys. Rev. Lett. **71**, 1994 (1993)

[CXRO] : http://henke.lbl.gov/optical_constants/

[Eidam 2010] Tino Eidam, Stefan Hanf, Enrico Seise, Thomas V. Andersen, Thomas Gabler, Christian Wirth, Thomas Schreiber, Jens Limpert, and Andreas Tünnermann
"Femtosecond fiber CPA system emitting 830 W average output power", Optics Letters **35**, 94 (2010)

[Emaury 2015] F. Emaury, A. Diebold, C. J. Saraceno, and U. Keller
"Compact extreme ultraviolet source at megahertz pulse repetition rate with a low-noise ultrafast thin-disk laser oscillator", Optica **2**, 980 (2015)

[Falcone 83] R.W. Falcone and J. Bokor,
"Dichroic beam splitter for extreme UV and visible radiation", Opt. Lett. **8**, 21 (1983)

[Ferray 88] M. Ferray, A. L'Huillier, X. F. Li, L. A. Lompre, G. Mainfray, and C. Manus,
"Multiple-harmonic conversion of 1064 nm radiation in rare gases", J. Phys. B **21**, L31 (1988).

[Hädrich 2011] S. Hädrich, M. Krebs, J. Rothhardt, H. Carstens, S. Demmler, J. Limpert and A. Tunnermann.
"Generation of μW level plateau harmonic at high repetition rate", Opt. Expr. **19**, 19374 (2011).

[Hädrich 2014] S. Hädrich, A. Klenke, J. Rothhardt, M. Krebs, A. Hoffmann, O. Pronin, V. Pervak, J. Limpert and A. Tunnermann.
"High photon flux table-top coherent extreme-ultraviolet source", Nature Photonics **8**, 779 (2014)

[Heyl 2012] C.M. Heyl, J. Gudde, A. L'Huillier, and U. Hofer,
"High order harmonic generation with μJ laser pulses at high repetition rates" J. Phys. B **45**, 074020 (2012)

[Kazamias 2003] S. Kazamias, D. Douillet, F.Weihe, C. Valentin, A. Rousse, S. Sebban, G. Grillon, F. Auge, D. Hulin, and Ph. Balcou
"Global optimization of high order harmonic emission", Phys. Rev. Lett. **90**, 193901 (2003).

[Kazamias 2011] S.Kazamias, S. Daboussi, O. Guilbaud, K. Cassou, D. Ros, B. Cros, and G. Maynard.
"Pressure induced phase matching in high order harmonic generation", Phys. Rev. A **83**, 063405 (2011)

[Krebs 2013] M. Krebs, S. Hadrich, S. Demmler, J. Rothhardt, A. Zair, L. Chipperfield, J. Limpert, and A. Tunnermann
"Toward isolated attosecond pulses at megahertz repetition rates", Nat. Photon. **7**, 555 (2013).

[Lewenstein 1994] M. Lewenstein, Ph. Balcou, M. Yu. Ivanov, 't Anne L'Huillier, and P. B. Corkum
"Theory of high-harmonic generation by low-frequency laser fields", Phys Rev A **49**, 2117 (1994)

[Lindner 2003] F. Lindner, W. Stremme, M. G. Schatzel, F. Grasbon, C. G. Paulus, H. Walther, R. Hartmann, and L. Struder
"High order harmonic generation at a repetition rate of 100 kHz", Phys. Rev. A **68**, 013814 (2003)

[Loch 2011] R.A. Loch, A. Dubrouil, R. Sobierajski, D. Decsamps, B. Fabre, P. Lidon, R.W.E. Van de Kruijs, F. Boekhout, E. Gullikson, J. Gaudin, E. Louis, F. Bijkerk, E. Mevel, S. Petit, E. Constant, Y. Mairesse.
" Phase characterization of the reflection on an XUV multilayer : comparison between attosecond metrology and standing wave measurements",Optic Letters **36**, 3386 (2011).

[Loriot 2015] V. Loriot, A. Marciniak, L. Quintard, V. Despre, B. Schindler, I. Compagnon, B. Concina, G. Celep, C. Bordas, F. Catoire, E. Constant and F. Lepine,
"Resolving XUV induced femtosecond and attosecond dynamics in polyatomic molecules with a compact attosecond beamline". Journal of Physics: Conference Series **635,** 012006 (2015)

[Mc Pherson 1987] A. McPherson, G. Gibson, H. Jara, U. Johann, T. S. Luk, I. A. McIntyre, K. Boyer, and C. K. Rhodes
"Studies of multiphoton production of vacuum-ultraviolet radiation in the rare gases", JOSAB **4** 595 (1987).

[Mevel 2000] E. Mevel, E. Constant, D. Garzella, P. Breger, C. Dorrer, C. Le-Blanc, F. Salin and P. Agostini
"Optimizing high order harmonic generation in absorbing gases", AIP-Conference-Proceedings **525**, 373-84 (2000)

[Nillon 2009] J. Nillon, S. Montant, J. Boullet, R. Desmarchelier, Y. Zaouter, E. Cormier and S. Petit
"15-fs-1µJ-100kHz by Direct Seeding of a NOPA and Its Fiber Pump by a CEP-Stabilized Oscillator", CLEO/Europe paper CF4.2THU, Munich (2009)

[Poletto 2004] L. Poletto, S. Bonora, M. Pascolini, and P. Villoresi
"Instrumentation for analysis and utilization of extreme ultraviolet and soft X-ray high order harmonics", Rev. Scient. Instr. **75**, 4413 (2004).

[Popmintchev 2008] Tenio Popmintchev, Ming-Chang Chen, Oren Cohen, Michael E. Grisham, Jorge J. Rocca,Margaret M. Murnane, and Henry C. Kapteyn
"Extended phase matching of high harmonics driven by mid-infrared light" , Opt lett **33**-2128 (2008)

[Rothhardt 2014] J. Rothhardt, M. Krebs, S. Hädrich, S. Demmler, J. Limpert, and A. Tünnermann
« Absorption-limited and phase-matched high harmonic generation in the tight focusing regime », New Journal of Physics **16**, 033022 (2014)

[Rundquist 1998] Andy Rundquist, Charles G. Durfee III, Zenghu Chang,
Catherine Herne, Sterling Backus, Margaret M. Murnane, Henry C. Kapteyn
"Phase-Matched Generation of Coherent Soft X-rays", Science **280**, 1412 (1998)

[Steingrube 2009] D. S. Steingrube, T. Vockerodt, E. Schultz, U. Morgner and M. Kovacev
"Phase matching of high order harmonics in a semi-infinite gas cell", Phys. Rev. A 80, 043819 (2009).

[Sutherland 2004] J.R. Sutherland, E.L. Christensen, N.D. Powers, S.E. Rhynard, J.C. Painter, and J. Peatross,
"High harmonic generation in a semi infinite gas cell", Opt. expr. **12**, 4430 (2004)

[Zaouter 2008] Y. Zaouter, J. Boullet, E. Mottay and E. Cormier
“Transform-limited 100 µJ, 340 MW pulses from a nonlinear-fiber chirped-pulse amplifier using a mismatched grating stretcher–compressor”, Opt. let. **33**, 1527 (2008)

[Wang 2014] He Wang, Yiming Xu, Stefan Ulonska, Joseph S. Robinson, Predrag Ranitovic & Robert A. Kaindl.
“Bright high-repetition-rate source of narrowband extreme-ultraviolet harmonics beyond 22 eV” . Nat. Commun. **6**:7459 (2015).

[Winterfeldt 2008] C. Winterfeldt, Ch. Spielmann, and G. Gerber,
“Optimal control of high-harmonic generation”, Rev. mod. phys. **80**, 117 (2008)